



Erasmus MC
Version: 1.0.00
Released: 2025-09-30



[Reader's Guide](#)

[Model Purpose](#)

[Model Overview](#)

[Assumption Overview](#)

[Parameter Overview](#)

[Component Overview](#)

[Output Overview](#)

[Results Overview](#)

[Key References](#)

MIcrosimulation SCreening ANalysis Gastric Cancer Model (MISCAN-Gastric): Model Profile

Erasmus University Medical Center

Contact

Duco Mulder (d.t.mulder@erasmusmc.nl)

Suggested Citation

Mulder DT, O'Mahony J, Sun D, van Duuren L, van den Puttelaar R, Harlass M, Han W, Huang R, Spaander MCW, Ladabaum U, Lansdorp-Vogelaar I.. MIcrosimulation SCreening ANalysis Gastric Cancer Model (MISCAN-Gastric): Model Profile. [Internet] Sep 30, 2025. Cancer Intervention and Surveillance Modeling Network (CISNET). Available from: <https://cisnet.cancer.gov/resources/files/mpd/gastric/CISNET-gastric-miscan-gc-model-profile-1.0.00-2025-09-30.pdf>

Version Table

Version	Date	Notes
1.0.00	2025-09-30	Initial release



[Reader's Guide](#)
[Model Purpose](#)
[Model Overview](#)
[Assumption Overview](#)
[Parameter Overview](#)
[Component Overview](#)
[Output Overview](#)
[Results Overview](#)
[Key References](#)

Reader's Guide

Core Profile Documentation

These topics will provide an overview of the model without the burden of detail. Each can be read in about 5-10 minutes. Each contains links to more detailed information if required.

Model Purpose

This document describes the primary purpose of the model.

Model Overview

This document describes the primary aims and general purposes of this modeling effort.

Assumption Overview

An overview of the basic assumptions inherent in this model.

Parameter Overview

Describes the basic parameter set used to inform the model, more detailed information is available for each specific parameter.

Component Overview

A description of the basic computational building blocks (components) of the model.

Output Overview

Definitions and methodologies for the basic model outputs.

Results Overview

A guide to the results obtained from the model.

Key References

A list of references used in the development of the model.



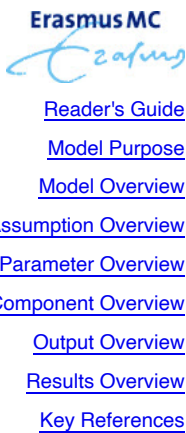
Erasmus MC
Model Purpose

Model Purpose

The Microsimulation Screening Analysis (MISCAN) gastric model is designed to evaluate the effect of gastric cancer screening and prevention strategies. These include endoscopic screening and *H. pylori* screen-and-treat interventions. MISCAN-gastric is developed within the Early Detection & Screening programme in the Department of Public Health at the Erasmus University Medical Center in Rotterdam, the Netherlands¹.

References

1. JDF Habbema, GJ Van Oortmarsen, JTN Lubbe, PJ Van der Maas. The MISCAN simulation program for the evaluation of screening for disease. Computer methods and programs in biomedicine. 1985;20(1):79–93.



Model Overview

As MISCAN-gastric is a microsimulation model, the model simulates independent individual life histories from birth until death, rather than as proportions of a cohort. This structure is similar across all MISCAN models, such as MISCAN-colon¹. This allows future state transitions to depend on past transitions, giving individuals a memory function. Unlike most traditional Markov models, MISCAN-gastric does not use yearly/monthly transition probabilities. Instead, in each health state, individual durations to other health states are generated. The term stochastic implies that model uses probability distributions and durations to simulate events, rather than using fixed values. The results are therefore subject to random variation. In MISCAN-gastric, some individuals develop precursor lesions which eventually progress to cancer.

MISCAN-gastric's natural history model is based on Correa's cascade, encompassing the states of atrophic gastritis (AG), intestinal metaplasia (IM), dysplasia, and ultimately carcinoma (Main Figure 1)². A distinction between limited (non-extensive) and extensive IM was incorporated to permit future assessment of surveillance strategies based on the extent of IM, which often features in clinical guidelines³.

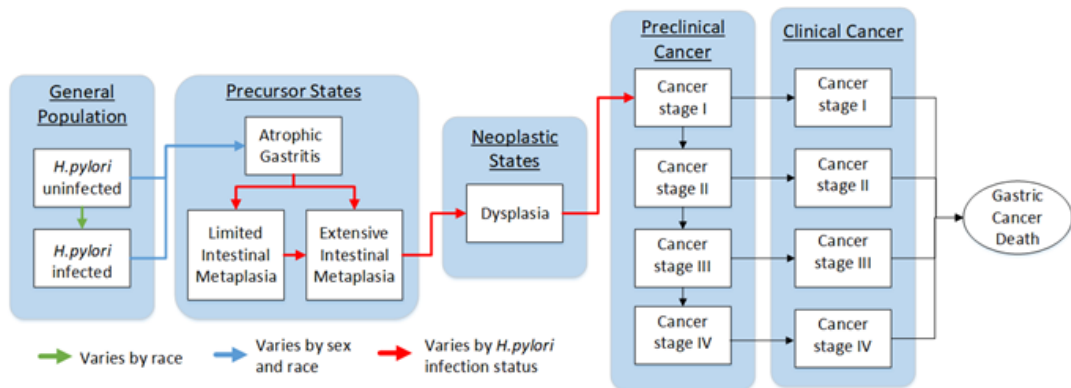


Figure 1: Natural history of the MISCAN-gastric model.

The arrows represent transitions between health states. The duration between transitions varies by race, sex and/or *H. pylori* infection status, depending on the color of the arrow.

H. pylori, *Helicobacter Pylori*.

References

1. R van den Puttelaar. Advancing Colorectal Cancer Screening: Challenges and Innovations [phdthesis]. Erasmus University; 2025.
2. P Correa. Human gastric carcinogenesis: a multistep and multifactorial process. *Cancer research*. 1992;52(24):6735–6740.
3. S Gupta, D Li, HB El Serag, others. AGA clinical practice guidelines on management of gastric intestinal metaplasia. *Gastroenterology*. 2020;158(3):693–702.



Erasmus MC

[Reader's Guide](#)
[Model Purpose](#)
[Model Overview](#)
[Assumption Overview](#)
[Parameter Overview](#)
[Component Overview](#)
[Output Overview](#)
[Results Overview](#)
[Key References](#)

Assumption Overview

The model employs several assumptions, primarily due to insufficient data on precursor lesions in asymptomatic populations¹. First, we assumed identical progression rates across racial groups. In contrast, the onset of precursor lesion was assumed to vary by race and sex. Second, *H. pylori* could elevate GC risk through two mechanisms: through an increased likelihood of developing precursor lesions (onset) or an accelerated progression of these lesions. The calibration decided how much each contributed. Regardless of the specific mechanism, the effect was assumed to be identical for all sex- and racial subgroups. Third, race-specific prevalence of *H. pylori* was based on estimates derived from literature and NHANES data². Finally, we assumed the same stage distribution at clinical diagnosis across racial groups, consistent with SEER data.

Mathematically, the onset age of precursor lesions was based on an *H. pylori*-specific hazard and race- and sex-specific generalized logistic hazard functions (blue arrows in Figure 2). The dwell times of health states followed Weibull distributions (red and black arrows in Figure 2), similar to the approach in other cancer natural history models^{3,4}. These transitions will now be further explained mathematically in the sequence of the model according to figure 2.

Atrophic gastritis onset risk

The onset age of precursor lesions was based on an *H. pylori*-specific hazard H_{H_p} and a race- and sex-specific generalized logistic hazard functions. The hazard for individuals uninfected with *H. pylori* was set to one. The logistic hazard function was rewritten for interpretability. We define a constant:

$$b_{s,r} = \frac{\log\left(\frac{1}{v_{s,r}}\left(\frac{K_{s,r}}{L}\right)^v - \frac{1}{v_{s,r}}\right)}{G_{s,r}^m - M_{s,r}},$$

To define the onset, based on random number x :

$$\text{Onset age}_i(x) = \frac{K_{s,r}}{\left(1 + v_{s,r} \times \exp(-b_{s,r}(x - M_{s,r}))\right)^{1/v_{s,r}}}.$$

Where L is a small number larger than 0 (0.001).

Calibrated parameters: $K_{s,r}$, $v_{s,r}$, $M_{s,r}$, $G_{s,r}^m$ for each sex s (male and female) and race r (black and white). x follows an exponential distribution with an *H. pylori* specific Hazard rate.

The parameters can be interpreted as follows:

- $K_{s,r}$ refers to the horizontal asymptote of the function.
- $v_{s,r}$, reflects the steepness in the inflection point.
- $M_{s,r}$ is the age of the inflection point
- $G_{s,r}^m$ is the age for which the function form equals L (0.001)

Atrophic gastritis progression:

Two independent dwell times are drawn from a Weibull distribution with varying means $k_{AG,1}$ and $k_{AG,2}$ but the same scale parameter λ_{AG} :

$$\text{Dwell AG}_1 \sim WB(k_{AG,1} * \Omega_{AG}^{I\{H_p\}}, \lambda_{AG})$$

$$\text{Dwell AG}_2 \sim WB\left(k_{AG,2} * \Omega_{AG}^{I\{H_p\}}, \lambda_{AG}\right),$$

where $\Omega_{AG}^{I\{H_p\}}$ represents the effect of *Helicobacter pylori* (*H. pylori*) on the mean progression time. $\Omega_{AG}^{I\{H_p\}}$ is a calibrated factor between 0 and 1, depending on *H. pylori* infection.

If $AG_1 \leq AG_2$, the individual progresses to limited intestinal metaplasia (IM). Otherwise, they progress to extensive IM directly.

Calibration parameters: $k_{AG,1}$, $k_{AG,2}$, λ_{AG} , $\Omega_{AG}^{I\{H_p\}}$

IM progression:

For limited IM, a dwell time to extensive IM is drawn from a Weibull distribution:

$$Dwell\ limited\ IM \sim WB(k_{IM\ lim} * \Omega_{IM/dys}^{I\{H_p\}}, \lambda_{IM})$$

For extensive IM, we draw a dwell time to dysplasia with a different mean, but the same scale parameter:

$$Dwell\ extensive\ IM \sim WB(k_{IM\ ext} * \Omega_{IM/dys}^{I\{H_p\}}, \lambda_{IM})$$

The parameter $\Omega_{IM/dys}^{I\{H_p\}}$ again represents the effect of *H. pylori* on the mean dwell time. Note that this effect is the same for IM and dysplasia.

To account for the effect of age on progression of disease, these dwell times are multiplied by a factor:

$$1 + \rho * age$$

Where age is the midpoint between the onset age of IM and the next state.

Calibration parameters: $k_{IM\ lim}$, $k_{IM\ ext}$, λ_{IM} , $\Omega_{IM/dys}^{I\{H_p\}}$, ρ

Dysplasia progression:

For dysplasia, we draw a dwell time to preclinical cancer stage 1 from a Weibull distribution:

$$Dwell\ dysplasia \sim WB(k_{dys} * \Omega_{IM/dys}^{I\{H_p\}}, \lambda_{dys})$$

Again, we account for the effect of age by multiplying the dwell times by $1 + \rho * age$, which is the same factor used in the dwell time of IM.

Additional calibration parameters: k_{dys} , λ_{dys} .

Preclinical cancer progression

In each preclinical cancer stage j , we draw a dwell time to preclinical stage $j+1$ from an exponential distribution:

$$Dwell\ cancer\ S_{j, j+1} \sim \exp(\lambda_j)$$

For $j=1,2,3$.

In each preclinical cancer stage, we also draw a dwell time until clinical detection:

$$Time\ until\ detection\ cancer\ S_j \sim \exp(\alpha_j)$$

For $j=1,2,3,4$

Preclinical cancers progress to the next stage if:

$$Dwell\ cancer\ S_{j, j+1} \leq Time\ until\ detection\ cancer\ S_j$$

Otherwise, cancers are clinically detected after the time until detection has elapsed.

Calibration parameters: λ_1 , λ_2 , λ_3 and α_1 , α_2 , α_3 , α_4

Calibration targets

The model was calibrated to SEER incidence data and data from studies. An overview of the data used from clinical studies can be found in Table 1.

Table 1: Data used in the calibration of MISCAN-gastric

Data used in calibration	Value (95% CI)	Reference
Total mean sojourn time (time between onset of preclinical cancer stage I and clinical diagnosis)	3.7 (1.96-8.28 years)	(13)
OR of non-cardia GC with <i>H. pylori</i> infection	4.79 (2.39-9.60)	(14)
Prevalence of <i>H. pylori</i> at age 35	White people: 36% Black people: 60%	(15)
Overall prevalence of atrophic gastritis	2.1% (0.7-4.7%)	(16)
Overall prevalence of intestinal metaplasia	9.1% (6.9-12.0%)	(16)
Overall prevalence of dysplasia	0.2% (0.04%-1.5%)	(17)
Odds ratio of developing precursor lesions of <i>H. pylori</i> + compared to <i>H. pylori</i> -	2.6 (1.5-3.3)	(16)
Odds ratios of intestinal metaplasia per age group	≤30 31-45 46-60 61-75 >75	Ref. 1.7 2.7 3.9 5.3
Odds ratios of developing precursor lesions for males compared to females	1.04	(18)
Proportion of extensive cases of all intestinal metaplasia cases	28%	(19)
Relative risk of intestinal metaplasia progression to subsequent precursors after <i>H. pylori</i> eradication	0.8	(20)
Relative risk of intestinal metaplasia progression to cancer following <i>H. pylori</i> eradication	0.7	(21)
Relative risk of atrophic gastritis progression to cancer following <i>H. pylori</i> eradication	0.28	(21)

References

1. RJ Huang, AR Ende, A Singla, others. Prevalence, risk factors, and surveillance patterns for gastric intestinal metaplasia among patients undergoing upper endoscopy with biopsy. Gastrointestinal endoscopy. 2020;91(1):70-77.e71.
2. RM Genta, A Sonnenberg. Characteristics of the gastric mucosa in patients with intestinal metaplasia. The American Journal of Surgical Pathology. 2015;39(5):700–704.
3. IMCM de Kok, J van Rosmalen, M van Ballegooijen. Description of MISCAN-cervix.
4. A. van der Steen, J. van Rosmalen, S. Kroep, others. Calibrating parameters for microsimulation disease models: a review and comparison of different goodness-of-fit criteria. Medical Decision Making. 2016;36(5):652–665.



Parameter Overview

An overview of the calibrated model parameters can be found in table 2.

Table 2: Calibrated values of the model parameters of MISCAN-gastric

Parameters	Interpretation	Calibrated Value
H_{Hp}	Hazard rate of developing atrophic gastritis for <i>H. pylori</i> infected individuals.	3.651151191
$K_{s,r}$	Horizontal asymptote of the onset age function	Black males: 0.135548 White males: 0.062793 Black females: 0.080278 White females: 0.083563
$v_{s,r}$	Inflection point of the onset age function	Black males: 19.54042 White males: 1.769942 Black females: 1.06667 White females: 1.242386
$M_{s,r}$	Age of the inflection point of the onset age function	Black males: 44.65589 White males: 46.55290 Black females: 52.38103 White females: 61.61536
$G_{s,r}^m$	Age for which the onset age function equals 0.001	Black males: 0.833748 White males: 8.716735 Black females: 1.437170 White females: 0.833748
$k_{AG,1}$	Weibull mean dwell time for atrophic gastritis to limited IM	23.43013009
$k_{AG,2}$	Weibull mean dwell time for atrophic gastritis to extensive IM	49.89100247
$\Omega_{AG}^{I\{Hp\}}$	Effect of <i>H. pylori</i> infection on progression time of atrophic gastritis	1
λ_{AG}	Scale of the Weibull distributions of atrophic gastritis dwell time	0.571882689
k_{IMlim}	Weibull mean dwell time for limited IM to extensive IM	74.07276355
$\Omega_{IM/dys}^{I\{Hp\}}$	Effect of <i>H. pylori</i> infection on the dwell time of IM and dysplasia	0.960589394
λ_{IM}	Scale of the Weibull distributions of IM dwell time	1.226024
k_{IMext}	Weibull mean dwell time for extensive IM to dysplasia	37.00643102
ρ	Parameter to model the effect of age on dwell time	7.980778226

Parameters	Interpretation	Calibrated Value
k_{dys}	Weibull mean dwell time for dysplasia to preclinical cancer stage 1	4.388887775
λ_{dys}	Scale of the Weibull distribution of dysplasia dwell time	0.661216
λ_j	Exponential distribution mean dwell time for preclinical cancer stage j to j+1	j=1: 3.297144 j=2: 0.794827 j=3: 1.137446
α_j	Exponential distribution mean dwell time for preclinical cancer to become clinically detected in stage j	j=1: 8.087736 j=2: 3.714227 j=3: 4.306321 j=4: 0.428254
$T_{H_p,AG}$	Multiplication factor of remaining atrophic gastritis dwell time after <i>H. pylori</i> eradication	3.554993
$T_{H_p,IM/dys}$	Multiplication factor of remaining IM and dysplasia dwell time after <i>H. pylori</i> eradication	1.125454



Component Overview

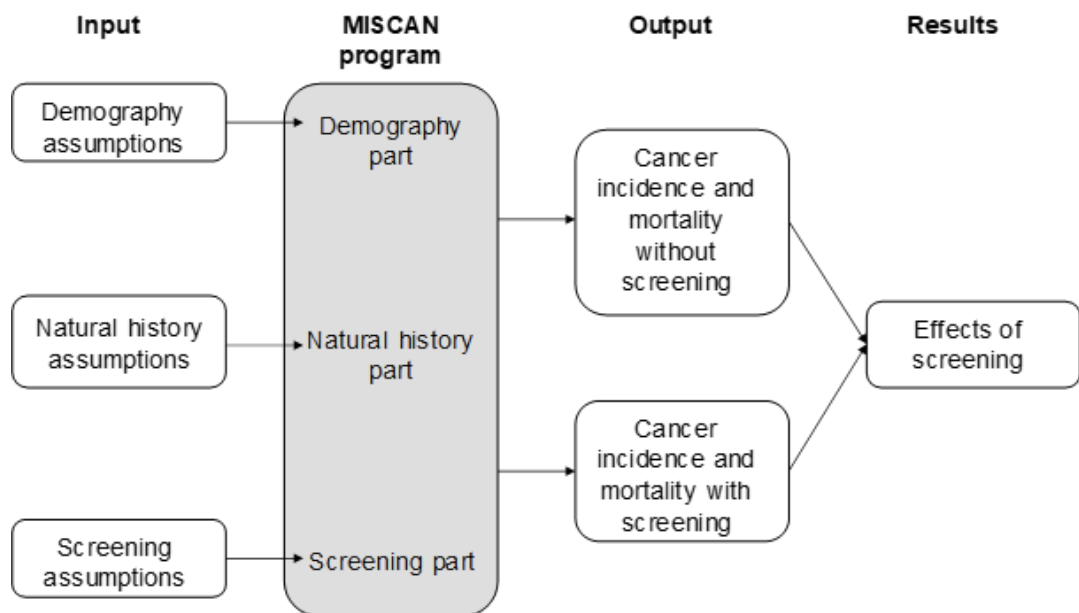


Figure 2: The structure of the MISCAN framework¹

The MISCAN-framework consists of three modules: demography, natural history and screening (Figure 1)¹. This framework has been extensively validated and applied for guiding cancer policy for other types of cancer in various contexts²⁻⁴. In the demography part, simulated individuals are born and die according to the population characteristics. The natural history part determines how many people develop precursor lesions and what proportion progresses to cancer. The screening part contains information about the screening test, such as the sensitivity and the effect of treatment. MISCAN models can be run with and without screening and prevention strategies. Comparing these scenarios can then inform the extent to which screening affects disease outcomes, such as incidence and mortality.

References

1. JDF Habbema, GJ Van Oortmarsen, JTN Lubbe, PJ Van der Maas. The MISCAN simulation program for the evaluation of screening for disease. *Computer methods and programs in biomedicine*. 1985;20(1):79–93.
2. F Van Hees, AG Zauber, H Van Veldhuizen, others. The value of models in informing resource allocation in colorectal cancer screening: the case of the Netherlands. *Gut*. 2015;64(12):1985–1997.
3. A Irzaldy, R Gvamichava, T Beruchashvili, others. Breast Cancer Screening in Georgia: Choosing the Most Optimal and Cost-Effective Strategy. *Value in Health Regional Issues*. 2024;39:66–73.
4. EAM Heijnsdijk, EM Wever, A Auvinen, others. Quality-of-life effects of prostate-specific antigen screening. *New England Journal of Medicine*. 2012;367(7):595–605.



Erasmus MC
Output Overview



[Reader's Guide](#)

[Model Purpose](#)

[Model Overview](#)

[Assumption Overview](#)

[Parameter Overview](#)

[Component Overview](#)

[Output Overview](#)

[Results Overview](#)

[Key References](#)

Output Overview

The outputs that can be generated by MISCAN-gastric include:

- Incidence counts of each disease by calendar year
- Mean prevalence of each disease state in five year age groups
- Number of invitations for screen tests
- Number of positive/negative tests
- Number of specific deaths and non-specific deaths
- Total number of life years and life years lost due to gastric cancer
- Number of life-years gained due to screening

Results Overview

Estimation of the number needed to screen (NNS) to prevent one death by race

One-time endoscopic screening with subsequent surveillance demonstrated optimal efficacy when initiated at age 50. The NNS for the overall US population was 3506 to prevent a NI-GC death. However, the NNS for the non-Hispanic black male population was as low as 621 (Figure 3).

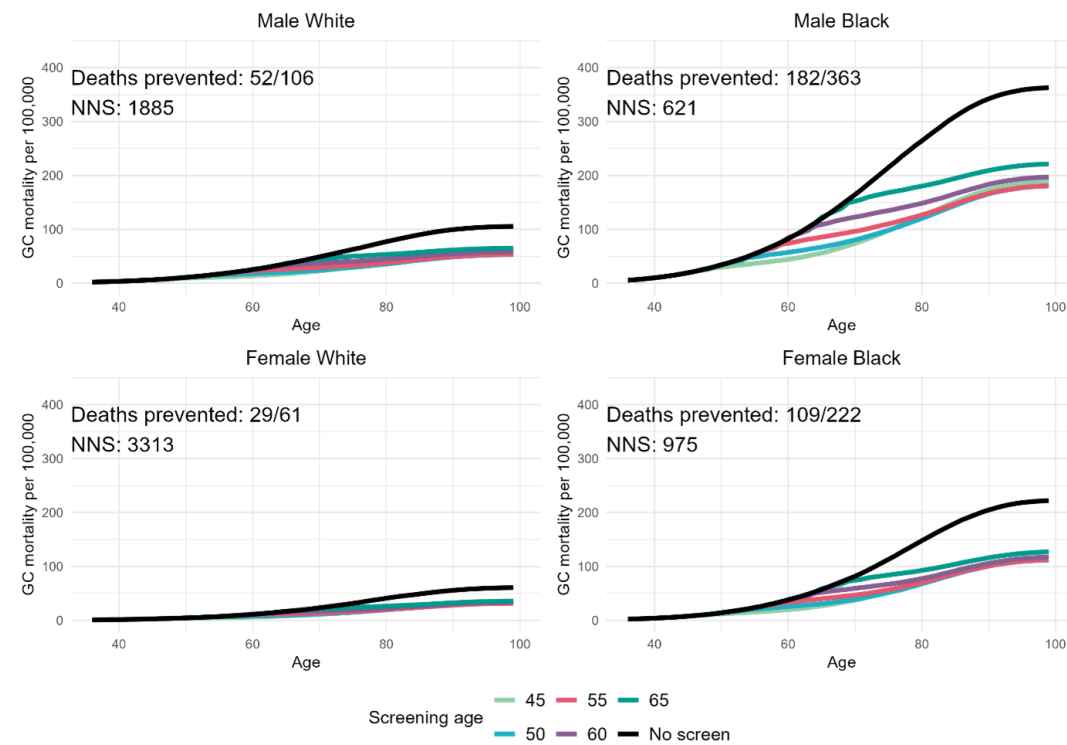


Figure 3: Effect of endoscopic screening on GC mortality

Optimal age of *H. pylori* screen-and-treat

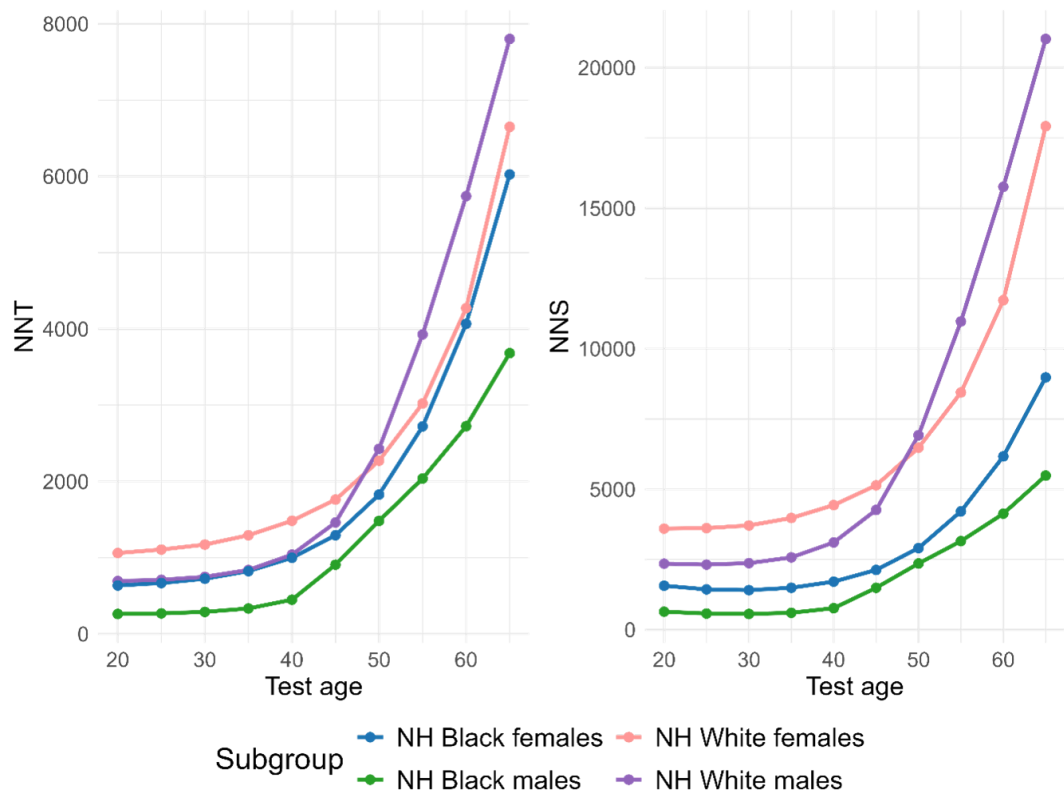


Figure 4: The Number Needed to Treat (NNT) and Number Needed to Screen (NNS) for *Helicobacter pylori* to prevent one case of gastric cancer. NH, non-Hispanic.



Erasmus MC
Key References



[Reader's Guide](#)
[Model Purpose](#)
[Model Overview](#)
[Assumption Overview](#)
[Parameter Overview](#)
[Component Overview](#)
[Output Overview](#)
[Results Overview](#)
[Key References](#)

Key References

P Correa. Human gastric carcinogenesis: a multistep and multifactorial process. *Cancer research*. 1992;52(24):6735–6740.

RM Genta, A Sonnenberg. Characteristics of the gastric mucosa in patients with intestinal metaplasia. *The American Journal of Surgical Pathology*. 2015;39(5):700–704.

S Gupta, D Li, HB El Serag, others. AGA clinical practice guidelines on management of gastric intestinal metaplasia. *Gastroenterology*. 2020;158(3):693–702.

JDF Habbema, GJ Van Oortmarsen, JTN Lubbe, PJ Van der Maas. The MISCAN simulation program for the evaluation of screening for disease. *Computer methods and programs in biomedicine*. 1985;20(1):79–93.

EAM Heijnsdijk, EM Wever, A Auvinen, others. Quality-of-life effects of prostate-specific antigen screening. *New England Journal of Medicine*. 2012;367(7):595–605.

RJ Huang, AR Ende, A Singla, others. Prevalence, risk factors, and surveillance patterns for gastric intestinal metaplasia among patients undergoing upper endoscopy with biopsy. *Gastrointestinal endoscopy*. 2020;91(1):70-77.e71.

A Irzaldy, R Gvamichava, T Beruchashvili, others. Breast Cancer Screening in Georgia: Choosing the Most Optimal and Cost-Effective Strategy. *Value in Health Regional Issues*. 2024;39:66–73.

IMCM de Kok, J van Rosmalen, M van Ballegooijen. Description of MISCAN-cervix.

R van den Puttelaar. Advancing Colorectal Cancer Screening: Challenges and Innovations [phdthesis]. Erasmus University; 2025.

A. van der Steen, J. van Rosmalen, S. Kroep, others. Calibrating parameters for microsimulation disease models: a review and comparison of different goodness-of-fit criteria. *Medical Decision Making*. 2016;36(5):652–665.

F Van Hees, AG Zauber, H Van Veldhuizen, others. The value of models in informing resource allocation in colorectal cancer screening: the case of the Netherlands. *Gut*. 2015;64(12):1985–1997.